Supplementary Information (SI) for Sustainable Energy & Fuels.
This journal is © The Royal Society of Chemistry 2025

Process Modelling and Thermodynamic Analysis of Hydrogen Production through Chemical Looping Ammonia Cracking

Supplementary information (SI)

1. Calculation of fixed E_{red} that cannot be utilised for hydrogen production

The fixed E_{red} defines the part of oxygen that was not reduced by hydrogen, in this process, Fe_2O_3 is partially reduced and Fe_3O_4 is formed. The ratio of fixed E_{red} can be calculated:

$$E_{redfix}(\%) = \frac{M_{O_2,\ total\ removed}}{M_{O_2,\ removed\ by\ Fe_3O_4}} = \frac{M_{Fe_2O_3} - M_{Fe}}{M_{Fe_2O_3} - M_{Fe_3O_4}}$$

where $M_{Fe_2O_3}$, $M_{Fe_3O_4}$, and M_{Fe} are the mass flow of circulated Fe_2O_3, Fe_3O_4, and circulated Fe. Therefore, $M_{O_2,\ total\ removed} = 500\ kg \cdot h^{-1}$ and $M_{O_2,\ removed\ by\ Fe_3O_4} = 4563\ kg \cdot h^{-1}$, so $E_{redfix} \approx 11\%$. About 11% of E_{red} is unutilised when T_{Ao} is 960 °C.

2. Calculation of $\dot{m}_{H_2,max}$ of the model at T_{Ao} = 960 °C

The molar flow of oxygen in feeding can be calculated:

$$F_{O_2} = \frac{M_{Fe_2O_3} - M_{RedOx}}{MW_{O_2}}$$

where $M_{Fe_2O_3} = 15180\ kg \cdot h^{-1}$ is the mass flow of Fe_2O_3, $M_{RedOx} = 13202\ kg \cdot h^{-1}$ is the mass flow of reduced oxides, and MW_{O_2} is the molar mass of O_2. Therefore, $F_{O_2} = 61.82\ kmol \cdot h^{-1}$.

Using Eq. (23), $F_{O_2}^{Fe_3O_4} = 15.61\ kmol \cdot h^{-1}$. Then using Eq. (22), $\dot{m}_{H_2,max} = 186.67\ kg \cdot h^{-1}$.

3. Calculation of M_{H_2} from Fe→Fe0.947O transition in Area-4

This calculation shows the highest yield that is possible in Area-4, where there are thermodynamic limitations for $Fe_{0.947}O \rightarrow Fe_3O_4$ transition, yielding no hydrogen from this. The only hydrogen yield is from Fe→ Fe_3O_4 transition.

The molar flow of Fe in the feeding can be calculated:

$$F_{Fe} = \frac{M_{OC} X_{Fe}}{MW_{Fe}}$$

where $M_{OC} = 18274\ kg \cdot h^{-1}$ is the mass flowrate of OC to SR, $X_{Fe} = 11.56\%$ is the mass fraction of Fe, and MW_{Fe} is the molar mass of Fe. Therefore, $F_{Fe} = 37.77\ kmol \cdot h^{-1}$.

Using Eq. (10) in SR, the mass flow of hydrogen can be calculated:

$M_{H_2} = 1.056 \cdot F_{Fe} MW_{H_2} = 80.56\ kg \cdot h^{-1}$

4. Calculations of η_{OEE}, η_{CGE} and ΔT_{SR}

A calculation is shown, using a SR pressure of 5 bar as an example.

When T_{Ao} is 960 °C, the model was converged with $M_{H_2} = 166.79\ kg \cdot h^{-1}$ and $M_{NH_3} = 1410\ kg \cdot h^{-1}$. The HHVs of ammonia and hydrogen are 22.5 MJ.kg^{-1} and 141 MJ.kg^{-1}, respectively. Therefore, using Eq. (20), $\eta_{CGE} = 74.13\%$.

The LHVs of ammonia and hydrogen are 18.8 MJ.kg^{-1} and 120 MJ.kg^{-1}, respectively. When SR pressure was 5 bar, $W_{comp} = 0$ and $Q_{process} = 0$. Therefore, using Eq. (19), $\eta_{OEE} = 75.51\%$.

The variation of O_2 in SR can be calculated:

$$\Delta M_{O_2 - SR} = \frac{M_{O_2,\ out} - M_{O_2,\ in}}{MW_{O_2}}$$

where $M_{O_2,\ in}$ and $M_{O_2,\ out}$ are the mass flow of oxides at SR inlet and outlet. Here, $\Delta M_{O_2 - SR} = 41.36\ kmol \cdot h^{-1}$. The variation of SR inlet and outlet temperature was 53.52 °C. Therefore, $\Delta T_{SR} = 1.294\ °C/kmol - O_2$.

5. Heat balance for the model

5.1 Calculation of the net heat consumed ($Q_{heat - sink}$) in heat sink

For the calculation, it is considered the following heat: the heat from input oxides (Q_i) and gas (Q_{NH_3}), the heat remained in output reduced oxides (Q_o) and direct loss (Q_v). Here, the values collected from the model (Fig. 8) were used.

The heat input of the heat sink can be calculated with:

$$Q_i = m_i C_{pi}(T_{Ao} - 25)$$

$$Q_{NH_3} = M_{NH_3} C_{p-NH_3}(T_{NH_3} - 25)$$

where $m_i = 20{,}000\ kg \cdot h^{-1}$ is the mass flow of FR inlet, $M_{NH_3} = 1{,}220\ kg \cdot h^{-1}$ is the mass flow of ammonia inlet. $C_{pi} = 1.57\ kJ \cdot kg^{-1} \cdot °C^{-1}$ is the mass-specific heat capacity of FR inlet from the model, $C_{p-NH_3} = 2.16\ kJ \cdot kg^{-1} \cdot °C^{-1}$ is the mass-specific heat capacity of ammonia gas. $T_{Ao} = 900\ °C$ and $T_{NH_3} = 153\ °C$. Therefore, $Q_i = 27400\ MJ \cdot h^{-1}$ and $Q_{NH_3} = 337.8\ MJ \cdot h^{-1}$.

The heat output of the heat sink can be calculated with:

$$Q_o = m_o C_{po}(T_{Fo} - 25)$$

where $m_o = 18{,}280\ kg \cdot h^{-1}$ is the mass flow of FR outlet, $C_{po} = 1.07\ kJ \cdot kg^{-1} \cdot °C^{-1}$ is the mass-specific heat capacity of FR outlet from the model and $T_{Fo} = 590\ °C$. Therefore, $Q_o = 11{,}073.1\ MJ \cdot h^{-1}$.

The heat loss in FR vent (Q_v) can be collected from the model, which is equal to 7,315.1 MJ·h^{-1}.

The net heat consumed in FR can then be calculated:

$$Q_{heat-sink} = Q_i + Q_{NH_3} - Q_o - Q_v = 9349.6\ MJ \cdot h^{-1}$$

5.2 Calculation of the net heat generated ($Q_{heat-source}$) in heat source

For the calculation, the following heat sources were considered: the heat from fuel-fraction of ammonia ($\Delta H^{o}_{CombNH_3-fuel}$) and the heat of oxidation of the steam in the SR (ΔH^{0}_{SR}). The heat losses from the AR and SR vent were considered to be 0, as the AR gas vent was cooled to 25 °C and the SR gas vent was cooled to be below zero in the model (Fig. 8).

The fuel-fraction of the mass flow of ammonia can be calculated using the equation below:

$$M_{NH_3-fuel} = M_{NH_3} - \frac{M_{H_2}}{0.178}$$

where $M_{NH_3} = 1{,}220\ kg \cdot h^{-1}$ is the mass flow of ammonia inlet (feed) and $M_{H_2} = 147.94\ kg \cdot h^{-1}$ is the mass flow of hydrogen output from the model. Here, $M_{NH_3-fuel} = 388.45\ kg \cdot h^{-1}$.

Using the equation below:

$$\Delta H^{o}_{CombNH_3-fuel} = HHV \cdot M_{NH_3-fuel} = 8470.1\ MJ \cdot h^{-1}$$

The heat of oxidation of the steam in the SR ($^{\Delta H^{0}_{SR}}$) can be collected from the model, which is equal to 757.7 MJ·h^{-1}.

The net heat generated in the SR and AR can then be calculated:

$$Q_{heat-source} = \Delta H^{o}_{CombNH_3-fuel} + \Delta H^{0}_{SR} = 9{,}497.8\ MJ \cdot h^{-1}$$

6. Stream composition

The table below (Table S1) summarises the gas composition of the outlet stream from the Fuel Reactor (FR).

Table S1 The gas composition of the outlet stream from the fuel reactor from the Aspen Plus model.

Gas	Molar fraction
NH_3	1.1410×10^{-11}
N_2	0.25
H_2	2.4524×10^{-5}
H_2O	0.748
O_2	1.9183×10^{-7}
NO_2	1.8261×10^{-12}
NO	1.2093×10^{-7}
N_2O	4.0931×10^{-12}

7. Techno-economic analysis

7.1 Estimation of major equipment cost (reactors)

The cost of each of the three reactors (FR, AR, and SR) (C_2), with a known capacity of S_2, was estimated based on the capacity of a similar reference equipment (S_1) of a known cost (C_1), using the following equation [1,2]:

$$C_2 = C_1 \left(\frac{S_2}{S_1}\right)^n \left(\frac{CEPCI_{Now}}{CEPCI_{Ref}}\right)$$

where n is the scaling factor (equal to 0.7), S_1 and S_2 are the oxide circulation rates, $CEPCI_{Now}$ is the current Chemical Engineering Plant Cost Index value (which is equal to 792 as of May 2024 [3,4]), and $CEPCI_{Ref}$ is the Chemical Engineering Plant Cost Index value of the reference equipment. The prices, CEPCI values, and oxide circulation rates of the three reference reactors are summarised in the table below (Table S2).

Table S2 Prices, CEPCI values, and oxide circulation rates of the reference reactors.

Equipment	Price (K$)	$CEPCI_{Ref}$	Circulation rate (ton/h)
Counter Current Reducer [5]	625	603 (2018) [3]	156
Fluidised Bed Reactor [6]	1550	395.6 (2002) [3]	120
Steam Reactor [7]	1650	609.5 (2019) [3]	4846

7.2 Estimation of miscellaneous equipment cost (heat exchanger and pump)

The cost of the heat exchangers (C_{HeatEx}) was estimated using the equation below [8]:

$$C_{HeatEx} = 2306.4\, A^{0.67}\, P^{0.28}$$

where A is the area of the heat exchanger in m^2 and P is the highest pressure in bar.

The cost of the pump (C_{Pump}) was estimated using the equation below [8]:

$$C_{Pump} = 2{,}268.13 \times 1.41\, P^{0.71} \left[1 + \frac{(1-0.80)^3}{(1-\eta_{Ex})^3}\right]$$

where η_{Ex} is the exergy efficiency of the pump and P is the power of the pump in kW. η_{Ex} was estimated using the equation below:

$$\eta_{Ex} = \frac{Exergy\ discharged}{W_{Pump}}$$

where W_{Pump} is the work of the pump in kW and physical exergy of the pump discharge was used, as obtained from the Aspen Plus model.

7.3 Estimation of Purchased Equipment Cost (PEC), Direct Costs (DC), Indirect Costs (IC), Total Capital Investment (TCI), Fixed Operating Cost (FOC), and Variable Operating Cost (VOC)

The PEC was calculated by summing the cost of all equipment costs (including reactors, heat exchangers, and pump). TCI, FOC, and VOC were estimated based on the PEC using the Peters and Timmerhaus Method [9]. The table below (Table S3) summarises the equipment costs calculated using the equations mentioned in the previous sections (section 7.1 and 7.2) and the corresponding PEC.

Table S3 Summary of equipment costs and the PEC.

Equipment	Price (K$)
Reactors	
Fuel Reactor	188
Air Reactor	885.3
Steam Reactor	46
Heat Exchangers	
Ammonia Pre-heater-1	5.1
Ammonia Pre-heater-2	5.1
Ammonia Vaporiser	21
Economiser	23.5
Steam Generator-1	11.8
Steam Generator-2	4.02
Air Heater	5.34
Pump	
DMW Pump	6.7
Total (PEC)	**1202**

The individual components used to estimate the DC and IC, as well as the TCI, FOC, and VOC calculated based on the PEC, are summarised in the tables below (Table S4 and Table S5).

Table S4 Calculation of DC, IC, TCI, FOC, and VOC.

Parameter	Assumption	Unit
Capacity Factor	90% [10]	
Scaling Factor	0.7 [7]	
Parasitic Power Requirement	13% of H_2 HHV [11]	
Power Cost	103.53 [12]	$
Cost of Renewable NH_3 (LCOA)	473 [13]	$.ton^{-1}
Interest rate & Plant Life	10	%
Plant Economic Life	25	Years
Direct Costs (DC) [9]		
Equipment Installation	0.39 PEC	
Instrumentation and Control	0.26 PEC	
Piping	0.30 PEC	
Electrical Systems	0.10 PEC	
Buildings	0.29 PEC	
Land & Yard Improvements	0.18 PEC	
Services & Facilities	0.55 PEC	
Total Direct Costs	**3.08 PEC**	
Indirect Costs (IC) [9]		
Engineering & Supervision	0.32 PEC	
Construction Expenses	0.34 PEC	
Legal Expenses & Contractor's fee	0.23 PEC	
Contingencies	0.37 PEC	
Total Indirect Costs	**1.26 PEC**	
Fixed Capital Investment = DC + IC	**4.34 PEC**	
Working Capital (WCI = 0.15FCI)	**0.65 PEC**	
TCI = WCI + FCI	**≈ 5 PEC**	
Fixed Operating Cost (FOC)	**0.01 TCI** [14]	
Variable Operating Cost (VOC)	**0.02 TCI** [14]	

Table S5 Summary of Capital Cost and Annual Expenditure.

Type	Cost (Million $)
Capital Investment	
Direct Capital Costs	3.69
Indirect Capital Costs	1.51
Fixed Capital Investment	5.20
Working Capital Investment	0.78
TCI	**5.98**
Annual Expenditure	
Fixed Operating Cost	0.06
Variable Operating Cost	0.12
Power Cost	0.0003
Annual Recovery	0.66
Ammonia (Feed)	4.55
Total Annualised Cost	**5.39**

7.4 Estimation of Levelised Cost of Hydrogen (LCOH)

The Levelised Cost of Hydrogen (LCOH) was estimated using the equations below:

$$LCOH = \frac{(CAPEX + Power_{Cost} + Heat_{Cost} + FOC + VOC)}{CF \times 8760 \times M_{H_2}}$$

$$CAPEX = TCI \times FCF$$

where $CAPEX$ is the annual Capital Expenditure, TCI is the Total Capital Investment, $Power_{Cost}$ is the cost of power input for the pump work (value shown in Table S4), $Heat_{Cost}$ is the cost of heat input (which is equal to 0), M_{H_2} is the hydrogen production rate in kg/h, CF is the capacity factor estimated considering a unit turn-around of 1 month ($CF = 0.916$), FCF is the Fixed Charge Factor, or fixed annual payment, estimated using the equation below, with an interest rate r (assumed to be 10%) and an economic life of the unit N of 25 years.

$$FCF = \frac{r\,(1+r)^N}{(1+r)^N - 1}$$

Based on a LCOA of \$473 ton^{-1} [13], the LCOH was calculated to be \$4.61 kg^{-1}. The contribution from each of the contributors to the LCOH (Levelised Cost of Ammonia (LCOA), annual CAPEX, FOC, VOC, and power cost) for the proposed process is shown in the figure below (Figure S1). The variations in their contribution were also evaluated for a series of LCOA, ranging from \$150 – 450 ton^{-1}, as shown in Figure S2.

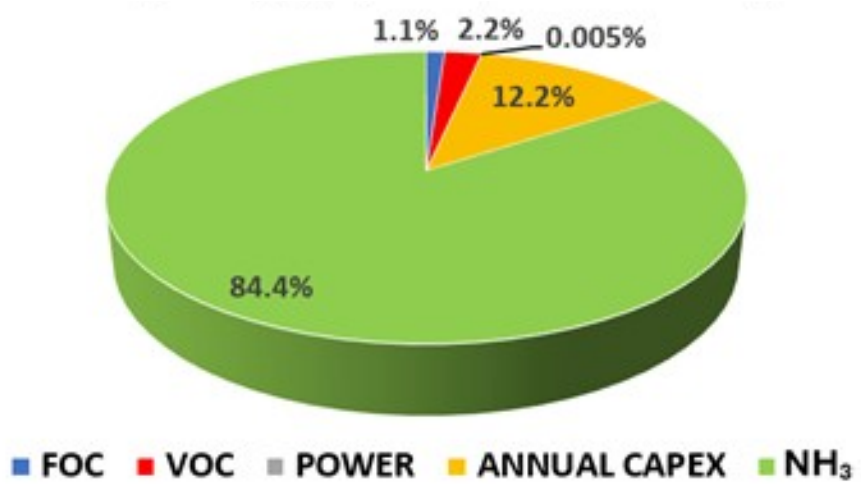


Figure S1 The contribution of the five contributors to the LCOH with a LCOA of \$473 ton^{-1}.

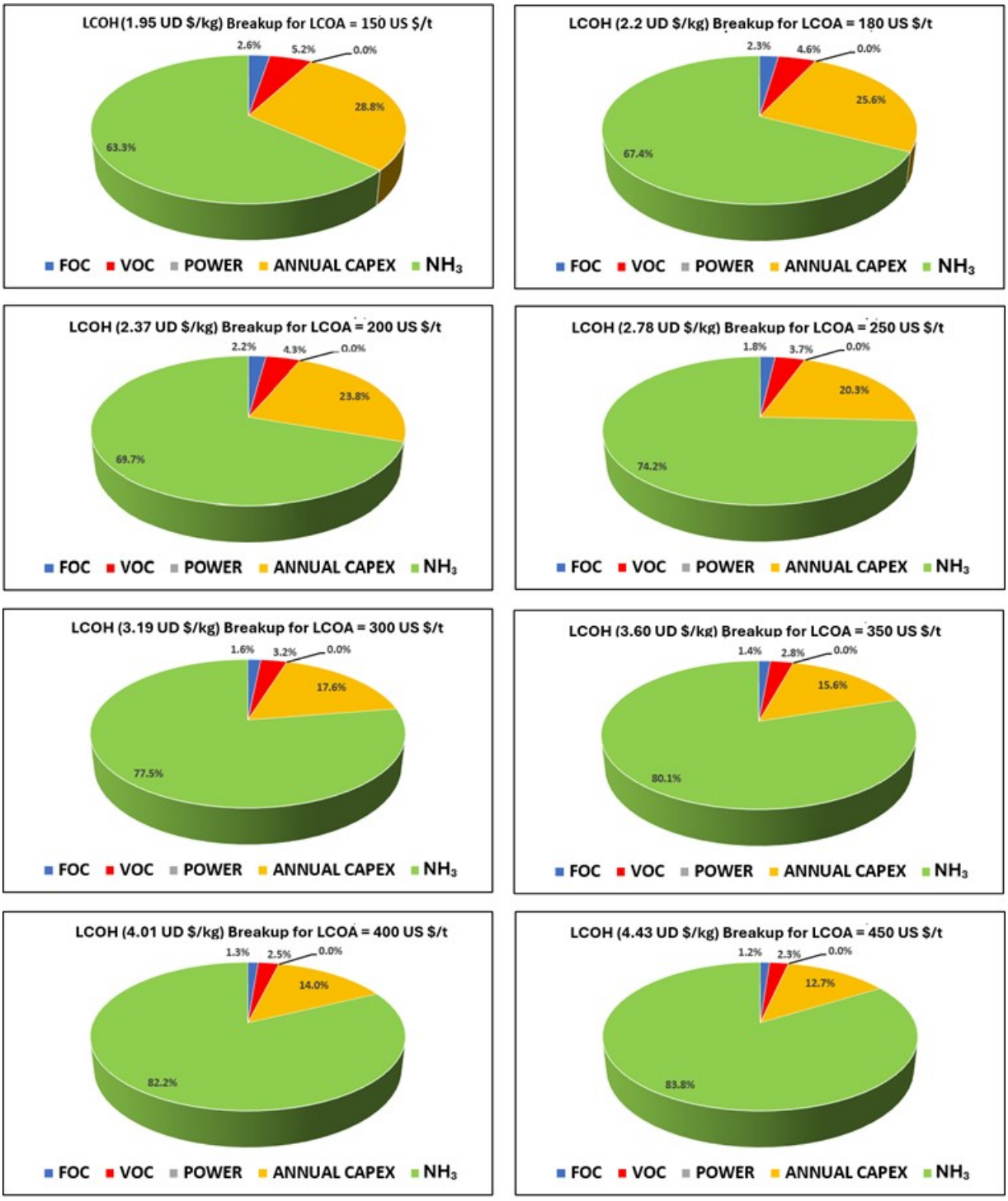


Figure S2 The contribution of the five contributors to the LCOH with different LCOA values.

It can be concluded that the largest contributor to the LCOH is the cost of the feed ammonia (over 60% for all cases), followed by the annual CAPEX, VOC, and FOC. The contribution of power cost is negligible. Future potential for large scale commercialisation of the process is immense, as significant reduction in the cost of ammonia is expected. For instance, studies revealed that the Levelised Cost of Ammonia (LCOA) can achieve \$310 ton^{-1} by 2030, and \$245 – 250 ton^{-1} by 2040, which can reduce the LCOH to \$3.1 - 3.7 kg^{-1} for ammonia CLCr processes.

References

[1] Kolmetz K, Jaya A, Ristiyanti R. Kolmetz Handbook of Process Equipment Design. KLM Technology Group; 2015.

[2] Khallaghi N, Hanak DP, Manovic V. Gas-fired chemical looping combustion with supercritical CO2 cycle. Appl Energy 2019;249:237–44. https://doi.org/10.1016/j.apenergy.2019.04.096.

[3] Manchester University. Chemical Engineering Plant Cost Index 2023. https://www.training.itservices.manchester.ac.uk/public/gced/CEPCI.html?reactors/CEPCI/index.html (accessed October 9, 2025).

[4] Jenkins S. 2024 CEPCI updates: May (prelim.) and April (final) 2024. https://www.chemengonline.com/2024-cepci-updates-may-prelim-and-april-final/ (accessed October 9, 2025).

[5] Zhang Q, Joshi RK, Xu D, Tong A, Fan L-S. A novel moving bed chemical looping process with integration of combustor heat exchangers for hydrogen production: Process simulation and techno-economic analysis. Int J Hydrogen Energy 2024;49:823–39. https://doi.org/10.1016/j.ijhydene.2023.07.300.

[6] Nexant Inc. Equipment Design and Cost Estimation for Small Modular Biomass Systems, Synthesis, Gas Cleanup, and Oxygen Separation Equipment. San Francisco: 2006.

[7] Khan MN, Shamim T. Techno-economic assessment of a chemical looping reforming combined cycle plant with iron and tungsten based oxygen carriers. Int J Hydrogen Energy 2019;44:11525–34. https://doi.org/10.1016/j.ijhydene.2019.03.109.

[8] Gabbrielli R, Singh R. Economic and Scenario Analyses of New Gas Turbine Combined Cycles With No Emissions of Carbon Dioxide. J Eng Gas Turbine Power 2005;127:531–8. https://doi.org/10.1115/1.1850492.

[9] Peters M, Timmerhaus K, West R. Plant Design and Economics for Chemical Engineers. 5th ed. Mc Graw Hill India; 2011.

[10] Arnaiz del Pozo C, Sánchez-Orgaz S, Navarro-Calvo A, Jiménez Álvaro Á, Cloete S. Integration of Chemical Looping Combustion in the Graz Power Cycle. Energies (Basel) 2024;17:2334. https://doi.org/10.3390/en17102334.

[11] Trading Economics. United Kingdom Electricity Price 2024. https://tradingeconomics.com/united-kingdom/electricity-price (accessed October 9, 2025).

[12] Mukherjee S, Kumar P, Yang A, Fennell P. Energy and exergy analysis of chemical looping combustion technology and comparison with pre-combustion and oxy-fuel combustion technologies for CO2 capture. J Environ Chem Eng 2015;3:2104–14. https://doi.org/10.1016/j.jece.2015.07.018.

[13] Hatton L, Bañares-Alcántara R, Sparrow S, Lott F, Salmon N. Assessing the impact of climate change on the cost of production of green ammonia from offshore wind. Int J Hydrogen Energy 2024;49:635–43. https://doi.org/10.1016/j.ijhydene.2023.10.117.

[14] Hanak DP, Jenkins BG, Kruger T, Manovic V. High-efficiency negative-carbon emission power generation from integrated solid-oxide fuel cell and calciner. Appl Energy 2017;205:1189–201. https://doi.org/10.1016/j.apenergy.2017.08.090.



https://dspace.org/

Process modelling and thermodynamic analysis of hydrogen production through chemical looping ammonia cracking

Soman, Anantha Krishnan Vinayak; Wang, Siqi; Shen, Ziqi; Zhu, Mingming

2025-12-21
Royal Society of Chemistry (RSC)
https://doi.org/10.1039/d5se01010a
Soman AKV, Wang S, Shen Z, Zhu M. (2025) Process modelling and thermodynamic analysis of hydrogen production through chemical looping ammonia cracking. Sustainable Energy & Fuels, Volume 9, Issue 24, December 2025, pp. 6761-6771

Downloaded from a DSpace repository. https://dspace.org/